EEET ECOLOGICAL ENGINEERING & ENVIRONMENTAL TECHNOLOGY

Ecological Engineering & Environmental Technology 2024, 25(6), 54–65
https://doi.org/10.12912/27197050/186598
ISSN 2719-7050, License CC-BY 4.0

Received: 2024.03.15
Accepted: 2024.04.22
Published: 2024.05.01

Forecasting Land Use and Land Cover Changes in the Malaprabha Right Bank Canal Command Area through Cellular Automata and Markov Chain Modeling

M.S. Madhusudhan[1], A.V. Shivapur[1], H.J. Surendra[2*]

[1] Department of Civil Engineering, PG Centre, V.T.U, Belagavi, Karnataka, 590018, India
[2] Department of Civil Engineering, Atria Institute of Technology, Karnataka, 560024, India
* Corresponding author's e-mail: careof.indra@gmail.com

ABSTRACT

To formulate an effective growth management plan, it is imperative to comprehend the dynamic changes that transpire. This study focused on identifying such shifts spanning four decades, from 1990 to 2020, and utilized a GIS-integrated approach, employing cellular automata Markov chain model within TerrSet software for the MRBC area, to predict land use and land cover (LULC) for 2030. The accuracy evaluation of the classification method yielded overall accuracy percentages of 94.11%, 94.11%, 90.19%, and 94.12% for 1990, 2000, 2010, and 2020, respectively, accompanied by Kappa values of 0.921, 0.921, 0.895 and 0.922. The LULC map for 2020 was forecasted and compared to the actual map for validation, revealing a discrepancy of less than 5% in class distribution. The study findings indicated a 12.32% reduction in agricultural land (151.7 km^2) compared to the 1990 LULC map in the projected 2030 map. In this future scenario, the converted region is allocated to urban and barren land classes. Consequently, decision-makers are urged to take necessary measures to preserve agricultural land from conversion, ensuring the enduring sustainability of agriculture.

Keywords: LULC, cellular automata Markov chain model, GIS, TerrSet, prediction.

INTRODUCTION

The term land use and land cover (LULC) change encompasses all human-induced modifications to the Earth's surface. While human alterations to land for sustenance have occurred over millennia, the current rates, extents, and intensities of LULC changes surpass historical levels, leading to unprecedented impacts on ecosystems and environmental processes at local, regional, and global scales. Systemic variations in population growth, economic development, and physical factors such as topography, slope condition, soil type, and climatic conditions collectively influence LULC changes. Remote sensing (RS) techniques offer a cost-effective and accurate means of analyzing LULC changes, particularly beneficial for scientists in less developed nations utilizing open-source data to enhance their proficiency in RS and GIS techniques. Two notable considerations arise: firstly, LULC changes occur rapidly, especially in irrigated areas not covered by ground surveys; secondly, ground surveys are often prohibitively expensive. The current landscape necessitates advancements in methods for efficiently collecting and analyzing extensive LULC data over larger areas in shorter timeframes.

The primary objective is to assess the nature, significance, and pace of land area changes from 1990 to 2020, shedding light on the historical state of land cover to comprehend the dynamics and patterns of change. The primary drivers of change are population increase and urbanization, influencing not only demographic shifts but also socio-economic, environmental, and cultural dimensions. Limited land and soil resources face alterations due to population growth and evolving needs for agriculture, urban development, and industry.

Recognizing the intricacies and rates of LULC dynamics is crucial for effective resource management, planning, and regulation, especially since dynamics are closely linked to the overuse of natural resources and influenced by climate change, soil conditions, and topographical features.

Understanding the drivers and dynamics of LULC changes is pivotal for formulating sustainable strategies and informed planning decisions. Land change models, whether dynamic or static, spatial or non-spatial, deductive or inductive, pattern-based or agent-based, serve as valuable tools for environmental studies on LULC change. These models, calibrated and validated for projecting future changes, employ strategies like MLPNN-CA-MC within the TerrSet model, effectively simulating various forms of land cover based on physical and socio-economic data.

This study aimed to evaluate the pattern of LULC change in the Malaprabha Right Bank Command (MRBC) area and predict changes for the year 2030. Utilizing remote sensing data with Arc GIS software, LULC changes have been explored, and predictions were made using the cellular automata (CA) Markov chain model embedded in TerrSet software.

STUDY AREA

The Malaprabha River, a significant tributary of the Krishna River, encompasses a catchment area of 2564 km^2, and is regulated by the Malaprabha Dam, also known as Naviluteertha Dam or Renuka Sagara Dam, situated in Saundatti Taluka of Belgaum District, Karnataka (refer to Figure 1). The dam, one of the shortest in the region, forms a catchment that provides irrigation through canals on both banks, covering an expanse of 196,132 ha in Belgaum, Bagalkot, Gadag, and Dharwad Districts. The river eventually joins the Krishna River at Kudala Sangam in Bagalkot district. With an average annual rainfall of approximately 766 mm, the Malaprabha basin experiences climatic conditions ranging from humid to semi-humid.

The basin caters to the drinking water needs of three million people across three districts and major cities like Hubli and Dharwad. However, the basin faces challenges, such as reduced flow due to developmental activities in the catchment area and declining rainfall over time. This decrease in flow has led to a shortage of water supply for irrigation, particularly at the tail end of the canals. The dependable flow at 75 percent capacity is recorded at 1,857 MCM. The right bank canal, stretching over 142 km, covers a total area of 1231 km^2 in the MRBC area. The waterlogging and salinity issues are prevalent in this command area, attributed to the presence of heavy black cotton soils and insufficient natural sub-surface drainage facilities. The topography of the irrigable command area under MRBC is generally flat, with a ground slope ranging from 1 in 50 to 1 in 200. About 80% of the

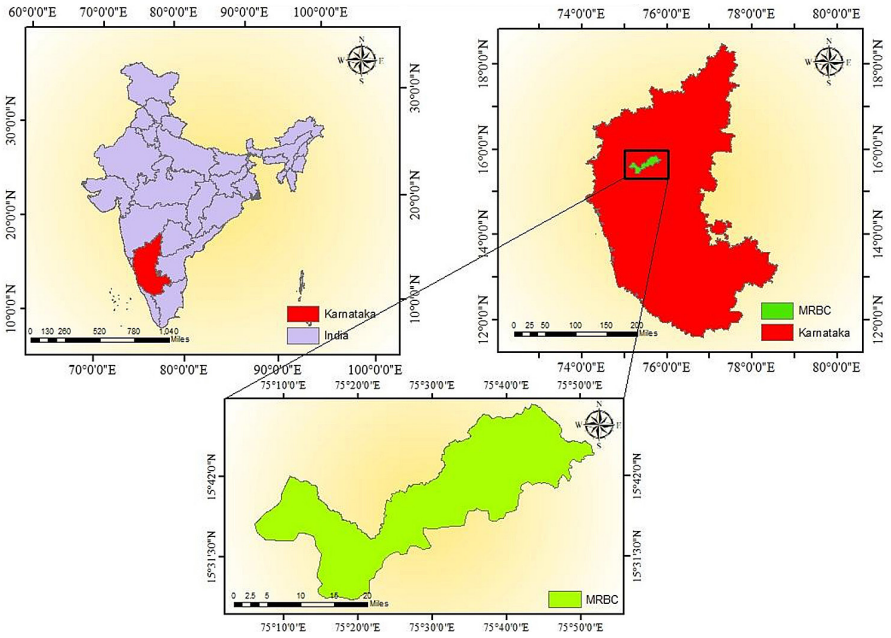

Figure 1. Location of the map of the study area

command area is covered by deep black cotton soils, and approximately 40% of the command area is characterized by saline alkali soil, locally known as KARL. This soil type results from extreme arid conditions, with low rainfall preventing the leaching of soluble salts.

The proportion of area allocated to Kharif and Rabi crops varies annually and by location, but on average, it is about 15 to 25% for Kharif crops and 75 to 85% for Rabi crops. The commonly cultivated crops in the MRBC area include Jowar, pulses, wheat, safflower, cotton, among others.

Data acquisition and data analysis

In this study, the primary data sources included a digital elevation model as well as satellite imagery from Landsat-5, Landsat-7, and Landsat-8, obtained through the USGS Earth Explorer. All imagery underwent geometric registration to align with the Universal Transverse Mercator (UTM43N) coordinate system. The land use and land cover information was derived from Landsat satellite imagery with a spatial resolution of 30×30 m, spanning the years 1990 to 2020. Additionally, Landsat satellite imagery was employed for detailed observations and classification of LULC changes throughout the study period (Figure 2).

Preprocessing of satellite image

Several image pre-processing operations, including atmospheric, geometric, and radiometric correction, have been conducted. Radiometric correction is a crucial step in the processing of satellite images, involving the conversion of digital numbers to radiance (or reflectance) values. This correction becomes imperative when working with measurements from multiple sensing platforms, such as the combination of Landsat-5, 7, and 8. Reflective band digital numbers (DNs) are transformed into top of atmosphere (TOA) reflectance by applying rescaling coefficients found in the metadata (MTL) file. The conversion is carried out using the formula provided below.

$$\rho_{\lambda'} = M_\rho Q_{cal} + A_\rho \quad (1)$$

where: $\rho_{\lambda'}$ – TOA planetary reflectance, M_ρ – band-specific multiplicative rescaling factor, A_ρ – band-specific additive rescaling factor, Q_{cal} – quantized and calibrated standard product pixel values (DN).

TOA reflectance with a correction for the sun angle is then:

$$\rho_\lambda = \frac{\rho_{\lambda'}}{Sin(SunElevation)} \quad (2)$$

Radiometric correction is applied to the each band in order to avoid the accumulation of errors while classifying the satellite images.

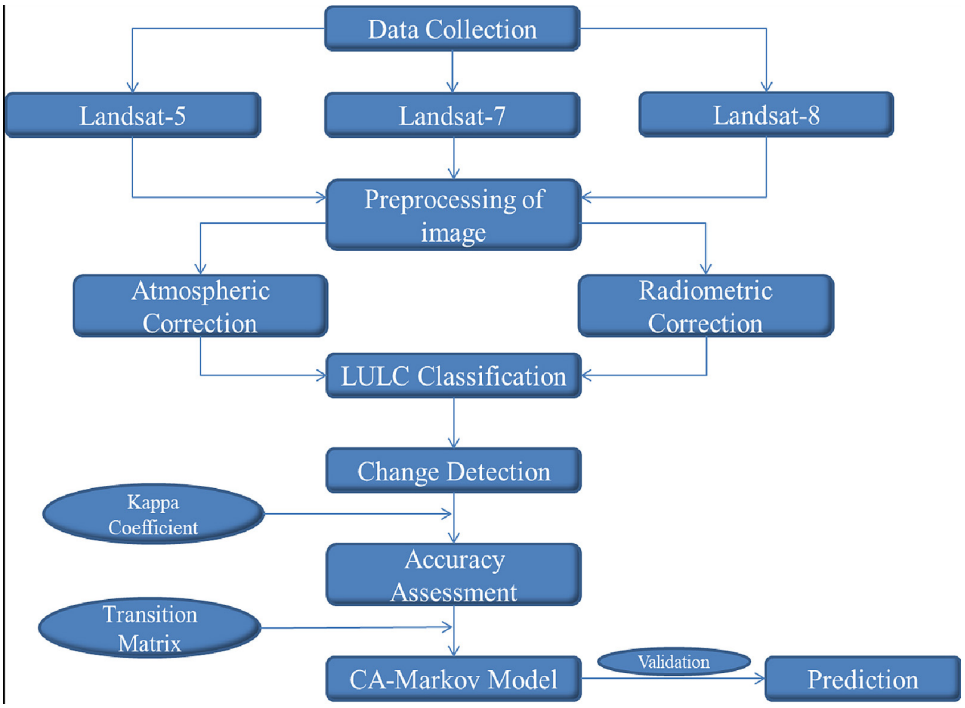

Figure 2. Wokflow process for predicting the LULC maps using CA-Markov chain model

Classification

After establishing a classification scheme, the implementation of maximum likelihood classification, renowned as one of the most widely used image classification techniques, was employed to generate maps encompassing various land use and land cover classes, utilizing training data. Subsequently, a field review was conducted to validate and verify uncertain areas. This ground check was facilitated with the assistance of GPS technology and local maps, as detailed by Mishra et al. (2020).

Land use/ land cover change detection

The importance of change identification lies in discerning transitions between different land-use classes. Commonly employed techniques for land change detection encompass image overlay, classification comparisons involving land cover metrics, change vector analysis, principal component analysis, image differencing, and the ratio of standardized difference vegetation index. In this study, the classification comparisons based on land cover metrics were utilized. The analysis focused on the specific regions of interest, scrutinizing each land cover type across different time periods.

Accuracy assessment

Accuracy assessment is conducted by comparing the generated map with reference data. This involves scrutinizing the relationship between ground truth and the outcomes of automated categorization through the use of error matrices. The error matrix provides various characteristics of classification performance, including errors of commission (inclusion) and omission (exclusion). These matrices are square, with the total number of columns and rows equal to the number of classes being assessed for accuracy.

Additionally, the Kappa coefficient is employed for precision evaluation. This coefficient serves as an indicator of the difference between the actual agreement achieved by an automated classifier and the reference data, as opposed to the chance agreement between a random classifier and the reference data. Kappa coefficient is calculated as:

$$Kappa\ coefficient\ (T) = \frac{(TS*TCS)-\sum(column\ total*row\ total)}{TS^2-\sum(column\ total*row\ total)} \quad (3)$$

where: *TS* – total samples, *TCS* – total corrected samples.

Validation and prediction of LULC maps

To project future developments in the command area, the study analyzed the trend variations of Land Use and Land Cover (LULC) changes for the years 1990, 2000, 2010, and 2020. The TerrSet model was employed to simulate future changes over time, utilizing the CA-MC stochastic modeling technique. Leveraging the transition probability matrix (TPM), the model predicts the

Table 1. Accuracy assessment of classified LULC map for 1990

Parameter	Urban	Barren land	Water body	Agriculture	Total (user)
Urban	12	0	0	0	12
Barren land	0	11	0	1	12
Water body	1	1	11	0	13
Agriculture	0	0	0	14	14
Total (producer)	13	12	11	15	51
OA = 94.11 %, K = 0.921					

Table 2. Accuracy assessment of classified LULC map for 2000

Parameter	Urban	Barren land	Water body	Agriculture	Total (user)
Urban	14	1	0	0	15
Barren land	1	11	0	0	12
Water body	0	0	11	0	11
Agriculture	0	1	0	12	13
Total (producer)	15	13	11	12	51
OA = 94.11 %, K = 0.921					

Table 3. Accuracy assessment of classified LULC map for 2010

Parameter	Urban	Barren land	Water body	Agriculture	Total (user)
Urban	12	0	0	0	12
Barren land	0	13	0	2	15
Water body	2	0	9	0	11
Agriculture	0	0	0	13	13
Total (producer)	14	13	9	15	51
OA = 90.19 %, K = 0.895					

Table 4. Accuracy assessment of classified LULC map for 2020

Parameter	Urban	Barren land	Water body	Agriculture	Total (user)
Urban	12	0	0	2	14
Barren land	0	13	0	0	13
Water body	0	0	13	0	13
Agriculture	0	1	0	10	11
Total (producer)	12	14	13	12	51
OA = 94.12 %, K = 0.922					

spatial organization of different LULC categories and scenarios (Li et al., 2015; Wang et al., 2012). The Markov matrix model utilizes the Bayes equation, comparing the initial (T1) and subsequent (T2) land cover states, to forecast LULC changes (Eastman et al., 2016). This approach allows for the anticipation of future LULC dynamics based on the observed patterns of change in the earlier years.

$$S(t+1) = Pij * S(t) \tag{4}$$

$$Pij = \begin{bmatrix} P11 & P12 & \ldots & P1n \\ P21 & P22 & \ldots & P2n \\ \ldots & \ldots & \ldots & \ldots \\ Pn1 & Pn2 & \ldots & Pnn \end{bmatrix} \tag{5}$$

where: $0 \leq Pij < 1$ and $\sum_{j=1}^{n} Pij = 1$,(i, j = 1, 2,…, n). The cellular automata model can be expressed by the following equation:

$$S(t,t+1) = f[S(t),N] \tag{6}$$

where: $S(t)$ and $S(t+1)$ are the system status at times t and $t + 1$, respectively, N – cellular field, t and $t+1$ are the different times, f – transformation rule of cellular states in local space, S – the set of limited and discrete cellular states, Pij—the transition probability matrix in a state (Leta M K et al., 2021).

The CA-Markov model proves to be a potent approach for simulating spatiotemporal dynamics by utilizing the transition probability matrices derived from the comparison of two distinct images. In contrast to the Markov chain model, where future changes primarily rely on the spatial condition of neighboring cells, the CA model introduces spatial and dynamic cycles. This integration of CA and Markov techniques is deemed adept at simulating and predicting land use and land cover changes. The resulting matrix captures the count of pixels undergoing changes in land use categories (Risma et al., 2019).

To project the 2030 LULC map, the 2020 LULC maps for the region were employed in simulating future LULC maps. As outlined by Araya and Cabral (2010) and Keshtkar and Voigt (2015), the models demonstrating accuracies exceeding 80% are considered highly reliable predictive tools. These findings affirm the CA-Markov model's credibility and effectiveness in forecasting LULC changes.

RESULTS AND DISCUSSION

The study findings initially deal with the classification of LULC with their accuracy assessment and the results of a change detection evaluation followed by the prediction of LULC maps.

Accuracy evaluation of the classified images

In this study, the performance of maximum likelihood classification (MLC) was evaluated

using key metrics, including overall accuracy, producer's accuracy, user's accuracy, and the Kappa statistic. For a quantitative assessment of classification accuracy, a random sample of 100 – plus points was selected. The overall accuracy rates for the land use and land cover maps in 1990, 2000, 2010, and 2020 are reported as 94.11%, 94.11%, 90.19%, and 94.12%, respectively, with a confidence level of 95%. Correspondingly, the Kappa statistics for the same years are 0.921, 0.921, 0.895, and 0.922.

According to Landis and Koch (1977), a Kappa statistic between 0.61 and 0.80 indicates substantial strength of agreement, while a range of 0.81 to 1.0 suggests almost perfect accuracy strength of assessment. In the present study, the calculated overall classification accuracy assessment falls within the almost perfect category, given the Kappa values ranging from 0.895 to 0.922.

Absolutely, it is a standard practice in the studies utilizing historical land use and land cover derived from remote sensing Landsat data to perform an accuracy assessment. As highlighted by Sitthi et al. (2016), this assessment involves the creation of a transition matrix that compares the classified map with a reference classification map. This matrix serves as a valuable tool in quantifying and evaluating the accuracy of LULC maps, providing insights into the reliability and precision of the classification process.

LULC change analysis

Land use categorization for the years 1990, 2000, 2010 and 2020 in the satellite images was conducted through the application of the MLC technique. The total land use area covers approximately 1231 km², constituting the cultivable command area on the right bank canal of Malaprabha. This area is further classified into four broad classes: water, agriculture, urban area, and Barren land. The outcomes are summarized in Table 5, revealing a discernible trend. The results indicate a consistent increase in the Urban and Barren land classes and a corresponding decrease in the agriculture class from 1990 to 2020**.**

The data presented in Table 5 clearly shows that agriculture is the predominant LULC type in the Malaprabha Right Bank Command, covering over 75% of the area consistently across all the years. The alterations in LULC have impacted the distribution of agricultural areas for the foreseeable future. The notable rise in barren land and urban areas has directly led to a reduction in agricultural land. The study's findings indicate that if adequate mitigations are not implemented, the same trend is expected to persist in the coming years.

Table 5. Comparison of LULC classes of 1990, 2000, 2010 and 2020 on basis of area wise in km²

No.	Classes	1990	2000	2010	2020
1	Urban	138.55	138.80	217.79	254.67
2	Barren land	37.85	44.89	45.12	56.94
3	Water body	1.22	1.18	1.33	3.44
4	Agriculture	1053.40	1046.15	966.78	915.98
Total		1231.02	1231.02	1231.02	1231.02

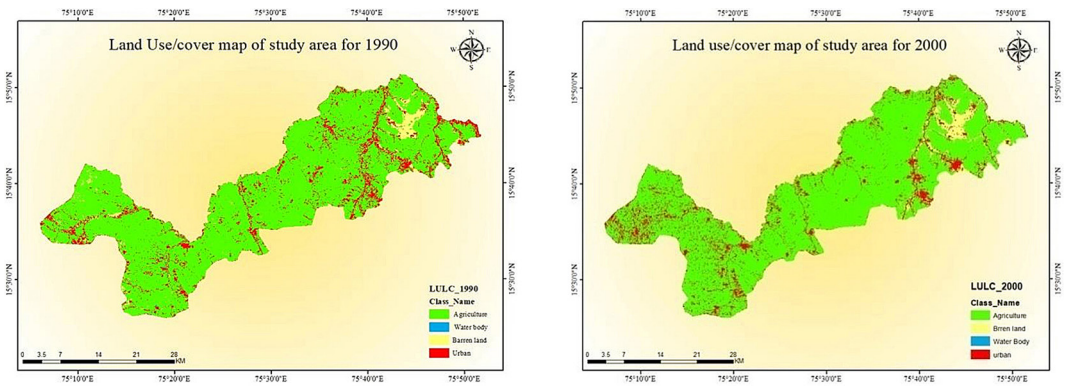

Figure 3. LULC map of MRBC for 1990 and 2000

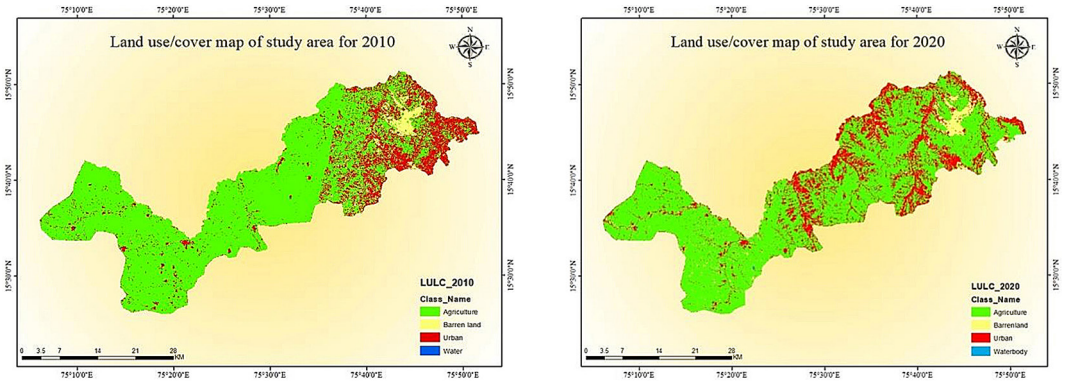

Figure 4. LULC map of MBRC for 2010 and 2020

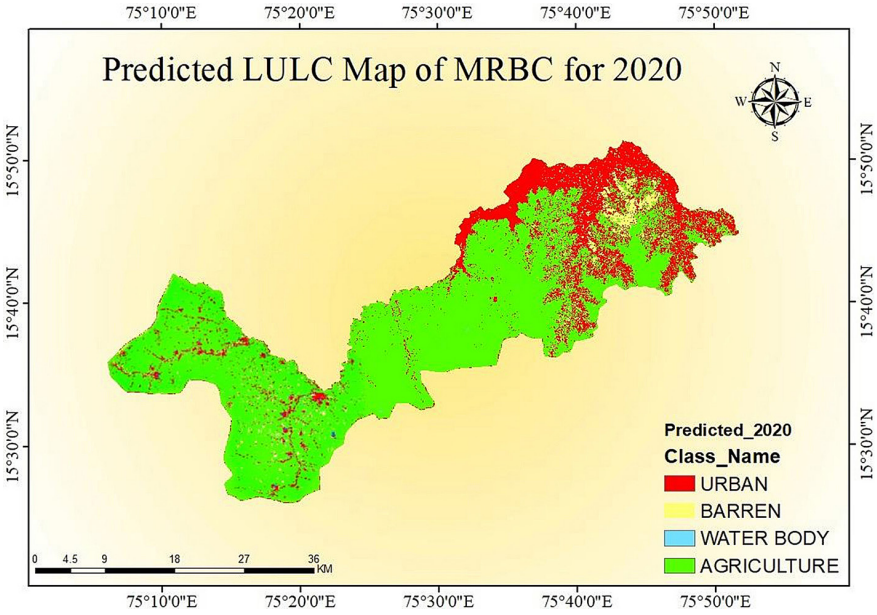

Figure 5. Predicted LULC map of MRBC for 2020

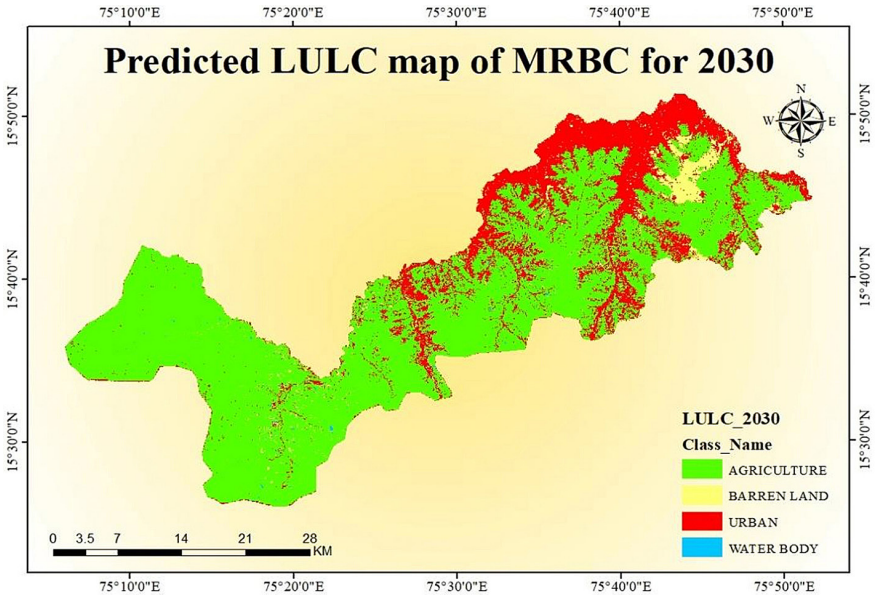

Figure 6. Predicted LULC map of MRBC for 2030

Transition probability matrix

This section discusses the transitions of land use and land cover areas between three classified images utilized in the study, presented in Table 6. The columns represent the LULC in 1990, and the rows indicate the LULC in 2000. Notable changes are observed in the 2000–2010 period, with a substantial conversion of agricultural areas into urban zones, amounting to nearly 80 km² in that decade alone. Similarly, from 2010 to 2020, there is a reduction in agricultural areas accompanied by an increase in urban and barren land. The potential reason for the shift from agricultural to barren and urban areas could be the limited availability of water sources for agricultural activities in the Malaprabha Right Bank Command area. The observed changes suggest a possible continuation of this trend in future years, an aspect that could be explored further through LULC prediction.

Validation of LULC between projected and classified land use

The international scientific community has extensively explored land cover change research, employing models that forecast future spatial patterns of change (Turner II et al., 1995; Lambin, 1997). Various modelers address this demand in different ways (Wilkie and Finn, 1988; Baker, 1989; Lambin 1997; Hall et al., 1995; Veldkamp and Fresco, 1996b; Geoghegan et al., 1997; Mertens and Lambin, 1997; Liverman et al., 1998), often integrating these models with raster-based Geographic Information Systems (GIS). Given the importance of assessing model accuracy in making predictions, scientists employ statistical methods to validate these models (Pontius, 2002).

The current study validates the projected future change map against the map of recent land cover change (2020) to establish the accuracy of the projected results obtained from the Markov process. The LULC for 2020 is projected using classified maps from 1990, 2000, and 2010, derived from Landsat satellite images. The methods for validating anticipated LULC, developed by Pontius et al. (2004) at Clark University in the United States, involve measuring the amount and location of land categories for prediction spanning decades at different resolutions. The comparison map, generated from the Markov model simulation results, is evaluated against a reference map representing reality (LULC map derived from Landsat image of 2020). The anticipated 2020 image is created using data from previous projections, and its accuracy is validated against the classified Land use of the actual 2020 year. To further validate the predicted map, it is overlaid with explanatory variables (e.g., distance from road, slope, and elevation maps, as shown in Figures 9, 10 and 11), utilizing the infrastructure class

Table 6. Transition matrix of LULC during years 1990–2000 (km²)

Year	1990					Total
	Classes	Water	Agriculture	Barren Land	Urban	
2000	Water	0.47	0.56	0.00	0.15	1.18
	Agriculture	0.43	949.58	10.12	86.02	1046.15
	Barren Land	0.00	20.70	19.89	4.30	44.89
	Urban	0.32	82.56	7.84	48.08	138.80
	Total	1.22	1053.40	37.85	138.55	1231.02

Table 7. Transition Matrix of LULC during years 2000–2010 (km²)

Year	2000					Total
	Classes	Water	Agriculture	Barren Land	Urban	
2010	Water	0.67	0.5	0.01	0.15	1.33
	Agriculture	0.37	867.52	8.55	90.34	966.78
	Barren Land	0.00	15.73	25.18	4.21	45.12
	Urban	0.14	162.4	11.15	44.10	217.79
	Total	1.18	1046.15	44.89	138.80	1231.02

Table 8. Transition matrix of LULC during years 2010–2020 (km^2)

Year	2010					Total
	Classes	Water	Agriculture	Barren Land	Urban	
2020	Water	0.94	2.15	0.01	0.33	3.43
	Agriculture	0.15	782.02	14.35	119.46	915.98
	Barren land	0.02	25.56	21.98	9.38	56.94
	Urban	0.22	157.05	8.78	88.62	254.67
	Total	1.33	966.78	45.12	217.79	1231.02

Table 9. Transition matrix of LULC during years 1990–2020 (km^2)

Year	1990					Total
	Classes	Water	Agriculture	Barren Land	Urban	
2020	Water	0.79	2.18	0.03	0.43	3.43
	Agriculture	0.27	847.90	13.04	54.77	915.98
	Barren land	0.03	27.67	19.7	9.54	56.94
	Urban	0.13	175.65	5.08	73.81	254.67
	Total	1.22	1053.4	37.85	138.55	1231.02

Table 10. Comparison of classified and modeled LULC of 2020 in km^2

No.	Class	Colour	Classified 2020 value	Predicted 2020 value	Error (km^2)	Error (%)
1	Agriculture	Green	915.98	911.34	4.64	0.51
2	Urban	Red	254.67	262.50	-7.83	-3.07
3	Barren land	Yellow	56.94	53.84	3.10	5.44
4	Water body	Blue	3.44	3.34	0.10	2.87

change tool under the IDRISI Selva environment. This additional step is taken to enhance the validation results for the 2020 Land use using the Markov Chain model.

The validation process, utilizing the Markov chain model as outlined in Table 10, involved a comparison between the model output for 2020 and the classified Land use of the same year. The examination revealed a minor disparity between the model and classified 2020 images, with barren land exhibiting the highest variation at + 5.44%. Error values between the classified LANDSAT image and the predicted TerrSet image (2020) were found to be 0.51% for agriculture, 2.87% for water bodies, and -3.07% for urban areas. Overall, the comparison of land use images indicated a variation of less than 5%, suggesting the Markov chain model produced a reasonably accurate prediction for the 2020 Land use. Consequently, the model has been employed to forecast land use and cover for the year 2030.

Prediction of 2030 land use and land cover image

Table 11 presents the Markov Chain model's forecast of future land use changes for the year 2030, while Table 12 displays area statistics for the years 1990, 2000, 2010, 2020, and the projected figures for 2030. Notably, there is a consistent reduction in agriculture area from 1990 to 2030, decreasing from 1053.40 km² in 1990 to 895.78 km² in 2030. This decline is anticipated in each decade, potentially influenced by urban

Table 11. Area statistics of predicted LULC classes of 2030

Class	Years 2030	
	Area (km^2)	Area (%)
Agriculture	901.70	73.25
Urban	273.06	22.18
Barren land	53.10	4.31
Water body	3.16	0.26

Table 12. Statistics of LULC area of 1990, 2000, 2010, 2020 and 2030

Years/Class	1990		2000		2010		2020		2030	
	Area (km^2)	Area (%)	Area (km^2)	Area (%)	Area (km^2)	Area (%)	Area (km^2)	Area (%)	Area (km^2)	Area (%)
Agriculture	1053.4	85.57	1046.15	84.98	966.78	78.53	915.98	74.41	901.70	73.25
Urban	138.55	11.25	138.80	11.27	217.79	17.69	254.67	20.69	273.06	22.18
Barren land	37.85	3.07	44.89	3.65	45.12	3.67	56.94	4.63	53.10	4.31
Water body	1.22	0.10	1.18	0.10	1.33	0.11	3.44	0.28	3.16	0.26

Table 13. Probability of changing LULC from 1990 to 2030 in area (km^2)

Year 2030	1990					Total
	Classes	Water	Agriculture	Barren Land	Urban	
2030	Water	0.71	1.95	0.02	0.48	3.16
	Agriculture	0.35	825.76	13.41	62.18	901.7
	Barren Land	0.02	23.69	19.36	10.03	53.1
	Urban	0.14	202	5.06	65.86	273.06
	Total	1.22	1053.4	37.85	138.55	1231.02

Table 14. Probability of changing LULC from 1990 to 2030 in percentage

Year	1990					Total (%)
	Classes	Water	Agriculture	Barren Land	Urban	
2030	Water	0.06	0.16	0.00	0.04	0.26
	Agriculture	0.03	67.08	1.09	5.05	73.25
	Barren land	0.00	1.92	1.57	0.81	4.3
	Urban	0.01	16.41	0.41	5.35	22.18
	Total	0.1	85.57	3.07	11.25	100%

expansion and a portion being transformed into barren land downstream.

Urban areas exhibit a rising trend from 1990 to 2030, driven by urbanization, settlement, and development, growing from 138.55 km^2 to 275.48 km^2, representing a percentage increase of approximately 11.13%. The percentage of water bodies is expected to remain constant in the predicted map, showing a gradual increase from 2020, stabilizing at 0.28%.

While the percentage of barren land increased from 3.07% in 1990 to 4.63% in 2020, it is projected to remain consistent at 4.57% in the next decade, covering an area of 56.32 km^2. The study suggests that the Markov chain model predicts a continued decrease in agriculture area, accompanied by an expansion of settlement and barren land. This trend is attributed, in part, to the inadequate availability of water at the canal's downstream, impacting its application for end-users. Notably, agriculture exhibits the highest likelihood of change, with a 67.08% probability of remaining in agriculture in 2030, while urban to urban transition remains stable at 5.35%. Conversely, the probabilities for water body and barren land transitioning to other classes are notably low. Specifically, the agriculture class demonstrates a considerable likelihood of transitioning to urban settlement (16.41%), with urban transitioning to agriculture at approximately 5.05%. Noteworthy changes include shifts from agriculture to barren land, urban to barren land, and barren land to agriculture, all indicating less than a 2% change in area. Consequently, the future outlook suggests a higher probability of change from agriculture to urban in 2030.

CONCLUSIONS

The primary objective of this study was to comprehend the evolution of historical and

projected land use and land cover patterns in the Malaprabha Canal's command area from 1990 to 2030. The classification results highlight a gradual increase in settlement and a concurrent decrease in agriculture from 1990 to 2020. The rate of change in these classes over each decade from 1990 to 2000 exhibits minimal fluctuations. However, a substantial shift occurs from 2000 to 2010, marked by a sharp decline in agriculture and a notable increase in urban settlement. This period coincides with significant urban development, likely contributing to the observed changes.

From 1990 to 2020, there is a consistent upward trend in barren land, a trend projected to continue into 2030 according to the CA-Markov model. This suggests a water scarcity issue, particularly at the canal's tail end, leading to a decline in agriculture and an expansion of barren and settlement areas. The land use classification by MLC demonstrates robust performance, with an overall Kappa statistic of a minimum of 0.895 and an overall classification accuracy exceeding 93.13%. The Markov model's predictions are further validated by the 2020 classified map generated by MLC.

The Markov model's forecasts indicate an escalating trend in settlement rates and a diminishing agricultural land area. The diminishing agricultural land may disrupt ecological balance in the future, while a growing population and expanding barren land underscore the increasing demand for food and water resources. The study predictions for the future land use and land cover of this developing region are crucial for developing informed management policies, especially concerning water resource allocation from the selected canal region.

Acknowledgement

The authors extend their heartfelt appreciation to Dr. R.V. Raikar, Dean R and D at K.L.E. Dr. M.S. Sheshgiri College of Engineering and Technology, Belagavi, and Dr. Vaibhav Chate, Associate Professor at KLS Gogte Institute of Technology, Belagavi, for their invaluable insights and guidance during the course of this research. Gratitude is also expressed to the entire staff of the Civil Engineering Department at PES College of Engineering, Mandya, Karnataka State, for their unwavering support throughout the research endeavor.

REFERENCES

1. Abbas, Z., Yang, G., Zhong, Y., Zhao, Y. 2021. Spatiotemporal Change Analysis and Future Scenario of LULC Using the CA-ANN Approach: A Case Study of the Greater Bay Area, China. Land. 10(6), 584.
2. Araya, Y.H., Cabral, P. 2010.Analysis and Modeling of Urban Land Cover change in Setubal and Sesimbra, Portugal.Remote Sensing, 2, 1549–1563.
3. Baker, W.L. 1989. A review of models of landscape change. Landscape Ecology, 2(2), 111–133.
4. Behera, M.D, Borate, S.N, Panda, S.N, Behera, P.R, Roy, P.S. 2012. Modelling and analyzing the watershed dynamics using Cellular Automata (CA)-Markov model—A geo-information based approach. Journal of Earth System Science, 121, 1011–1024.
5. Eastman, J.R. TerrSet Geospatial Monitoring and Modeling System—Manual. Available online: www.clarklabs.org (accessed on 2 January 2016).
6. Gautam, N.C. and Narayanan, L.R.A. 1983. Landsat MSS Data for Land Use/Land Cover Inventory and Mapping: A Case Study of Andhra Pradesh. Journal of Indian Society of Remote Sensing, 11, 15–28.
7. Geoghegan, J., Wainger, L.A. and Bocksael, N.E. 1997, Spatial landscape indices in a hedonic framework: An ecological economics analysis using GIS. Ecological Economics, 23, 251–264.
8. Gong, P et al. 2013. Finer Resolution Observation and Monitoring of Global Land cover: First Mapping Results With Landsat TM and ETM + Data. International journal of remote sensing, 34(7), 2607–2654.
9. Hall, D.K., Foster, J.L., Chien, J.Y.L. and Riggs, G.A. 1995, Determination of actual snow covered area using Landsat TM and digital elevation model data in Glacier National Park, Montana. Polar Record, 177(31), 191–198.
10. Landis, J.R., Koch G.G. 1977. The measurement of observer agreement for categorical data, Biometrics, Mar, 33(1), 159–174.
11. Keshtkar, H., Voigt, W. 2015. A spatiotemporal analysis of landscape change using an integrated Markov chain and cellular automata models A spatiotemporal analysis of landscape change using an integrated Markov chain and cellular automata models. Model. Earth Syst. Environ. 2(1), 1–13.
12. Lambin, E.F.1997. Modeling and Monitoring Landcover change processes in Tropical Regions. Progress in Physical Geography, 21, 375–393.
13. Leta, M.K., Demissie, T.A., Tränckner, J. 2021. Modeling and Prediction of Land Use Land Cover Change Dynamics Based on Land Change Modeler (LCM) in Nashe Watershed, Upper Blue Nile Basin, Ethiopia. Sustainability., 13(7), 3740. https://doi.org/10.3390/su13073740
14. Li, S.H., Jin, B.X., Wei, X.Y., Jiang, Y.Y., Wang, J.L.

2015. Using CA-Markov model to model the spatio-temporal change of land use/cover in Fuxian Lake for decision support. ISPRS Ann. Photogramm. Remote Sens. Spat. Inf. Sci. 2, 163–168.

15. Liverman, D., Moran E., Rindfuss R.R. and Stern P.C. 1998. People and Pixels: Linking Remote Sensing and Social Science (Washington, D.C.: National Academy Press). LongTerm Growth Prediction for San Francisco and Washington/Baltimore.
16. Maduako, I. and Wang, J. 2017. Spatio-temporal Urban Growth Dynamics of Lagos Metropolitan Region of Nigeria based on Hybrid methods for LULC Modeling and Prediction. European Journal of Remote Sensing. 51. https://doi.org/10.1080/22797254.2017.1419831.
17. Memarian, H., Kumar Balasundram, S., Bin Talib, J., Teh Boon Sung, C., Mohd Sood, A., Abbaspour, K. 2012. Validation of CA-Markov for simulation of land use and cover change in the Langat Basin, Malaysia. Journal of Geographic Information System. 4, 542–554.
18. Mertens, B. and Lambin, E.F. 1997. Spatial modeling of deforestation in Southern Cameroon. Applied Geography, 17(2), 143–162.
19. Mishra, V.N., Rai, P.K. 2016. A remote sensing aided multi-layer perceptron-Markov chain analysis for land use and land cover change prediction in Patna district (Bihar), India. Arabian Journal of Geosciences. 9, 1–18.
20. Noszczyk T. 2018. A review of approaches to land use changes modeling. Human and Ecological Risk Assessment. 25(6), 1377–1405.
21. Pontius Jr, R.G., Huffaker, D. and Denman, K. 2004, Useful techniques of validation for spatially explicit land-change models. Ecological Modeling, 179(4), 445–461.
22. Pontius Jr, R.G. 2002, Statistical methods to partition effects of quantity and location during comparison of categorical maps at multiple resolutions. Photogrammetric Engineering Remote Sensing, 68(10), 1041–1049.
23. Mishra, P. K., Rai, A., Rai S.C. 2020. Land use and land cover change detection using geospatial techniques in the Sikkim Himalaya, India. The Egyptian Journal of Remote Sensing and Space Science, 23(2), 133–143.
24. Risma, Zubair H. and Paharuddin. 2019. Prediction of land use and land cover (LULC) changes using CA-Markov model in Mamuju Subdistrict. Journal of Physics L Conference series 1341 082033.
25. Sananda Kundu, Deepak Khare, Arun Mondal. 2017. Landuse change impact on sub-watersheds prioritization by analytical hierarchy process (AHP), Ecological Informatics, 42, 100–113.
26. Serra, P., Pons, X., Saurí, D. 2008. Land-cover and land-use change in a Mediterranean landscape: A spatial analysis of driving forces integrating biophysical and human factors. Applied Geography, 28(3), 189–209.
27. Sitthi, A., Nagai, M., Dailey, M., Ninsawat, S. 2016. Exploring land use and land cover of geotagged social-sensing images using Naive Bayes Classifier. Sustainability, 8, 921.
28. Tong S.T.Y., Sun Y., Yang Y.J. 2012. Generating a future land-use change scenario: A case study of the Little Miami River Watershed, Ohio. Journal of Environmental Informatics. 19, 108–119.
29. Turner II, B.L., Skole, D., Sanderson, S., Fischer, G., Fresco, L., Leemans, R. 1995. Land-Use and Land-Cover Change, Science/Research Plan. IGBP Report No.35/HDP Report No.7, Stockholm, Sweden, and Geneva, Switzerland.
30. Veldkamp, T.A. and Fresco I.O. 1996b. CLUE-CR: an integrated multi-scale model tosimulate land use change scenarios in Costa Rica. Ecological Modeling, 91(1–3), 231–248.
31. Wang, S.Q., Zheng, X.Q., Zang, X.B. 2012. Accuracy assessments of land use change simulation based on Markov-cellular automata model. Procedia Environ. Sci. 13, 1238–1245. https://doi.org/doi:10.1016/j.proenv.2012.01.117.
32. Wilkie, D.S., and Finn, J.T. 1988. A Spatial Model Of Land Use and Forest Regeneration In The Ituri Forest of North Eastern Zaire. Ecological Modelling, 41, 307–323.
33. Zadbagher, E., Becek, K., Berberoglu, S. 2018. Modeling land use/land cover change using remote sensing and geographic information systems: Case study of the Seyhan Basin, Turkey. Environmental Monitoring Assessment. 190, 1–15.